JOURNAL OF MODERN OPTICS, 2016
VOL. 63, NO. 14, 1323–1330
http://dx.doi.org/10.1080/09500340.2016.1143052

Taylor & Francis
Taylor & Francis Group

Pump beam waist-dependent pulse energy generation in Nd:YAG/Cr^{4+}:YAG passively Q-switched microchip laser

Chao-yu Li and Jun Dong

Department of Electronic Engineering, School of Information Science and Engineering, Xiamen University, Xiamen, China

ABSTRACT

The incident pump beam waist-dependent pulse energy generation in Nd:YAG/Cr^{4+}:YAG composite crystal passively Q-switched microchip laser has been investigated experimentally and theoretically by moving the Nd:YAG/Cr^{4+}:YAG composite crystal along the pump beam direction. Highest pulse energy of 0.4 mJ has been generated when the Nd:YAG/Cr^{4+}:YAG composite crystal is moved about 6 mm away from the focused pump beam waist. Laser pulses with pulse width of 1.7 ns and peak power of over 235 kW have been achieved. The theoretically calculated effective laser beam area at different positions of Nd:YAG/Cr^{4+}:YAG composite crystal along the pump beam direction is in good agreement with the experimental results. The highest peak power can be generated by adjusting the pump beam waist incident on the Nd:YAG/Cr^{4+}:YAG composite crystal to optimize the effective laser beam area in passively Q-switched microchip laser.

ARTICLE HISTORY
Received 17 December 2015
Accepted 11 January 2016

KEYWORDS
Nd:YAG; Cr^{4+}:YAG; composite crystal; passively Q-switched; microchip laser

1. Introduction

Compact, passively Q-switched solid-state lasers with high beam quality and high peak power have potential applications in laser processing, engine ignition, efficient nonlinear frequency conversion, and so on [1–3]. Composite crystals have been widely used in constructing compact passively Q-switched miniature lasers by bonding Nd:YAG crystal and Cr^{4+}:YAG crystal together because they have mitigated the thermal effect and improved the beam quality and optical efficiency [4]. Passively Q-switched microchip lasers based on Nd:YAG/Cr^{4+}:YAG composite crystals and composite ceramics have been demonstrated [5,6]. Quasi-continuous-wave (QCW) laser diode working at low repetition rate has been demonstrated to be an effective method to provide high pump power intensity and alleviate the thermal effect of solid-state lasers. QCW laser diode-pumped Cr^{4+}:YAG passively Q-switched Nd:YAG micro laser with peak power of over 1 MW has been demonstrated [7]. Passively Q-switched laser pulses with pulse energy of 2.4 mJ and peak power of 2.8 MW have been achieved in QCW laser diode-pumped Nd:YAG/Cr^{4+}:YAG composite ceramics passively Q-switched laser [5]. The Nd:YAG/Cr^{4+}:YAG ceramic laser generated pulses with energy of 2.5 mJ, 1.3 ns pulse duration (FWHM), and peak power of 1.9 MW [8]. These QCW laser diode-pumped Nd:YAG/Cr^{4+}:YAG composite materials passively Q-switched lasers operated in several Hz to hundred kHz. High repetition rate laser operation of Nd:YAG/Cr^{4+}:YAG composite crystal was achieved under continuous-wave laser diode pumping and optical efficiency of 18% was achieved [9]. Comparable laser performance with pulse width of 237 ps and peak power of 0.72 W were also achieved in Yb:YAG/Cr^{4+}:YAG composite ceramic passively Q-switched microchip laser, the optical efficiency of 19% was obtained [10]. Recently, QCW laser diode-pumped Yb:YAG/Cr^{4+}:YAG composite crystal passively Q-switched laser with peak power over 1 MW has also been demonstrated [11]. The pulse energy generated in passively Q-switched microchip laser is proportional to the laser beam area according to the passively Q-switched laser theory [12]. The large laser beam area is a key issue to generate high pulse energy in end-pumped passively Q-switched microchip laser. The laser beam area in Cr^{4+}:YAG passively Q-switched Nd:YAG laser strongly depends on the incident pump beam waist and pump power. For the constant pump power, the incident pump beam waist and propagation of the pump beam inside the Nd:YAG crystal govern the inversion population distribution inside the Nd:YAG crystal for achieving large laser beam area. The effects of the laser diode pump beam spot size on laser threshold and efficiency of continuous-wave

CONTACT Jun Dong jdong@xmu.edu.cn

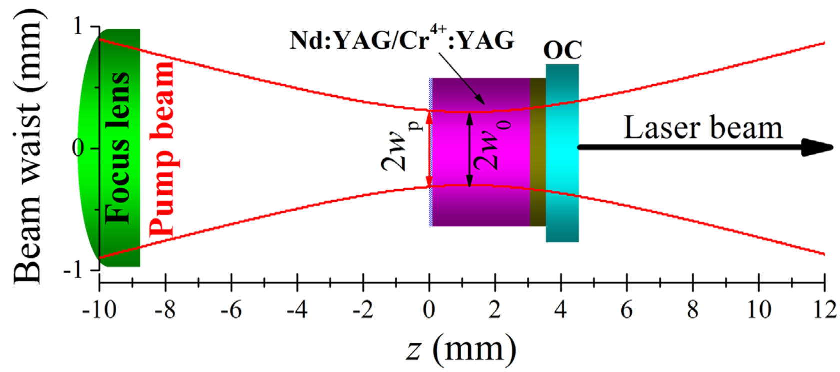

Figure 1. Schematic diagram of laser diode-pumped Nd:YAG/Cr^{4+}:YAG composite crystal passively Q-switched microchip laser. OC is the output coupler. w_0 is the focused pump beam waist and $w\mathbf{p}$ is the incident pump beam waist at z (the position of the Nd:YAG/Cr^{4+}:YAG composite crystal along the pump beam direction). (The colour version of this figure is included in the online version of the journal.)

solid-state laser have been investigated by varying the focused pump beam diameter [13,14]. The pump power threshold increases and the optical efficiency decreases with the pump beam spot [15–17]. However, up until now, there is no report on the investigation of the effects of the pump beam waist on the pulse energy in the passively Q-switched microchip lasers. The effects of the inversion population distribution under different pump beam waists and the nonlinear absorption of Cr^{4+}:YAG saturable absorber on the pulse energy generation in passively Q-switched microchip laser are worthy investigating.

In this paper, the effects of incident pump beam waist on pulse energy generation in the Nd:YAG/Cr^{4+}:YAG composite crystal passively Q-switched microchip laser have been investigated by moving Nd:YAG/Cr^{4+}:YAG composite crystal along the pump beam direction to change the pump beam waist incident on the Nd:YAG surface. The passively Q-switched pulse energy as a function of the position of the Nd:YAG/Cr^{4+}:YAG composite crystal along the pump beam direction has been studied and the optimal position of Nd:YAG/Cr^{4+}:YAG composite crystal along the pump beam direction for high pulse energy generation has been obtained experimentally. The variation of the effective laser beam area as a function of the position of the Nd:YAG/Cr^{4+}:YAG composite crystal along the pump beam direction is theoretically calculated and found that the theoretical simulation results are in good agreement with the experimental data.

2. Experiments

The schematic diagram of experimental setup for studying the effects of pump beam waist on the pulse energy in the QCW laser diode-pumped Nd:YAG/Cr^{4+}:YAG composite crystal passively Q-switched laser is shown in Figure 1. Nd:YAG crystal and Cr^{4+}:YAG crystal used for fabricating Nd:YAG/Cr^{4+}:YAG composite crystal were grown by Czochralski (CZ) method along the [1 1 1] direction. The Nd^{3+} ions' doping concentration of Nd:YAG crystal is 1 at.%, the thickness of Nd:YAG crystal is 3 mm. The thickness of Cr^{4+}:YAG crystal is 0.5 mm, the initial transmission of Cr^{4+}:YAG crystal is 80%. The Nd:YAG/Cr^{4+}:YAG composite crystal was fabricated using thermal bonding technology. The plane-parallel Nd:YAG/Cr^{4+}:YAG composite crystal was used as gain medium and also a saturable absorber. One surface of the Nd:YAG crystal was coated with anti-reflection at 808 nm and highly reflected at 1064 nm to act as the rear cavity mirror of the laser cavity. The Cr^{4+}:YAG crystal surface was coated with anti-reflection at 1064 nm to reduce the intracavity loss. Plane-parallel mirror with reflectivity (R_{OC}) of 60% at 1064 nm was attached tightly to Nd:YAG/Cr^{4+}:YAG composite crystal to act as the output coupler. The cavity length is 3.5 mm. A fiber-coupled 808 nm QCW laser diode from DILAS (M1F2S22-808.2-100C-IS9.2MPW) with core diameter of 200 μm and numerical aperture of 0.22 was used as the pump source. Two focus lenses with 8-mm and 11-mm focal lengths, respectively, were used to collimate and focus the pump beam on the Nd:YAG crystal. The diameter of the focused pump beam spot was measured to be 600 μm. The pump pulse duration of the QCW laser diode was fixed to 0.7 ms for effectively extracting the energy stored in Nd:YAG crystal. The pump repetition rate of the QCW laser diode was fixed to 10 Hz for alleviating the thermal effect of Nd:YAG crystal. The maximum incident pump peak power of the QCW laser diode after optical coupling system was measured to be 81 W. For studying the effect of the incident pump beam diameter ($2w_p$) on the pulse energy in the QCW laser diode end-pumped Nd:YAG/Cr^{4+}:YAG passively Q-switched microchip laser, the Nd:YAG/Cr^{4+}:YAG composite crystal was moved along the pump beam direction close to or away from the position of the focused pump beam diameter ($2w_0$). z represents the position of

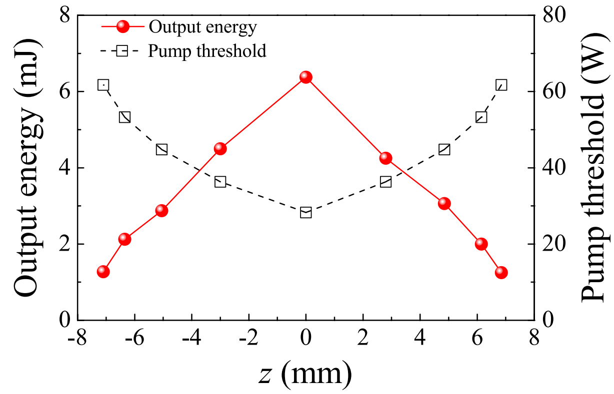

Figure 2. Output energy and pump power threshold of the Nd:YAG/Cr^{4+}:YAG composite crystal passively Q-switched microchip laser versus z (the position of the Nd:YAG/Cr^{4+}:YAG composite crystal along the pump beam direction). (The colour version of this figure is included in the online version of the journal.)

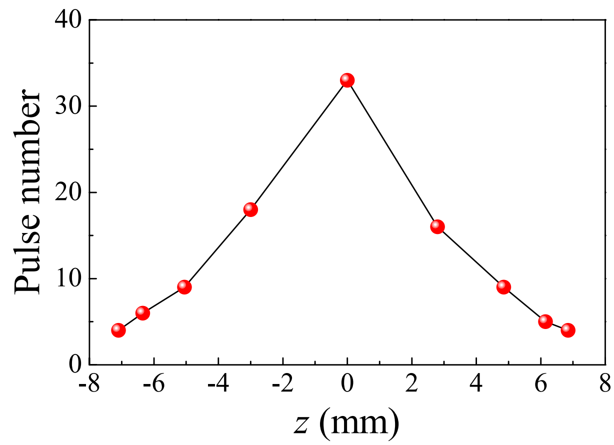

Figure 3. Laser pulses generated in the Nd:YAG/Cr^{4+}:YAG composite crystal passively Q-switched microchip laser versus z (the position of the Nd:YAG/Cr^{4+}:YAG composite crystal along the pump beam direction). (The colour version of this figure is included in the online version of the journal.)

the Nd:YAG/Cr^{4+}:YAG composite crystal along the pump beam direction. The Nd:YAG/Cr^{4+}:YAG composite crystal passively Q-switched lasers were operated at room temperature without active cooling. Average output power and pulse characteristics were measured with a Thorlab power meter and 6 GHz Tektronix digital oscilloscope (TDS6604), respectively.

3. Experimental results

The incident pump peak power from QCW laser diode after optical coupling system was fixed to 81 W for studying the performance of Nd:YAG/Cr^{4+}:YAG passively Q-switched laser under different pump beam waists. The output energy and the pump threshold of QCW laser diode-pumped Nd:YAG/Cr^{4+}:YAG composite crystal passively Q-switched laser as a function of the position of Nd:YAG/Cr^{4+}:YAG composite crystal along pump beam direction are shown in Figure 2. The highest output energy of Nd:YAG/Cr^{4+}:YAG composite crystal passively Q-switched microchip laser was obtained when the focused pump beam spot was located 1.2 mm inside the Nd:YAG crystal. $z = 0$ indicates the position of the Nd:YAG/Cr^{4+}:YAG composite crystal along the pump beam direction for generating highest output energy. The distance between entrance surface of Nd:YAG and the pump beam focus spot is 1.2 mm at $z = 0$, as shown in Figure 1. Negative displacement indicates that the Nd:YAG/Cr^{4+}:YAG composite crystal is close to the focus lens. Positive displacement indicates the Nd:YAG/Cr^{4+}:YAG composite crystal is far away from the focusing lens. The highest output energy of 6.4 mJ was achieved at $z = 0$; when the input pump energy of 56.7 mJ was applied, the corresponding optical efficiency was about 11.3%. The output energy decreased when the Nd:YAG/Cr^{4+}:YAG composite crystal was moved away from $z = 0$ for highest output energy generation. The decrease of the output energy with $|z|$ was attributed to the changing of the pump beam diameter, and mode matching between laser beam and pump beam. The inversion population decreased at the same pump peak power when the Nd:YAG/Cr^{4+}:YAG composite crystal was positioned further away from $z = 0$. The pump threshold at a certain position of Nd:YAG/Cr^{4+}:YAG composite crystal along the pump beam direction was measured by adjusting the pump power. The lowest pump threshold was also measured at $z = 0$, while the pump threshold increased when the Nd:YAG/Cr^{4+}:YAG composite crystal was moved away from $z = 0$. This is in good agreement with the variation of the pump threshold at different pump beam diameters in solid-state laser and semiconductor laser [13,14]. The pump threshold at $z > 0$ is higher than that at $z < 0$ for the same absolute value of z. This may be caused by the different inversion population distributions inside the Nd:YAG crystal and the thermal effect when the Nd:YAG/Cr^{4+}:YAG composite crystal is positioned along the pump beam direction with different incident pump beam waists.

The number of laser pulses generated in the QCW laser diode-pumped Nd:YAG/Cr^{4+}:YAG composite crystal passively Q-switched microchip laser varied with the position of the Nd:YAG/Cr^{4+}:YAG composite crystal along the pump beam direction. Figure 3 gives the variation of the pulse number with z. Thirty-three Q-switched laser pulses were generated at $z = 0$, the number of laser pulses decreased with $|z|$. The number of laser pulses generated in Nd:YAG/Cr^{4+}:YAG composite crystal passively Q-switched microchip laser at $z > 0$ is less than that at $z < 0$ for the same distance moved away from $z = 0$. The incident

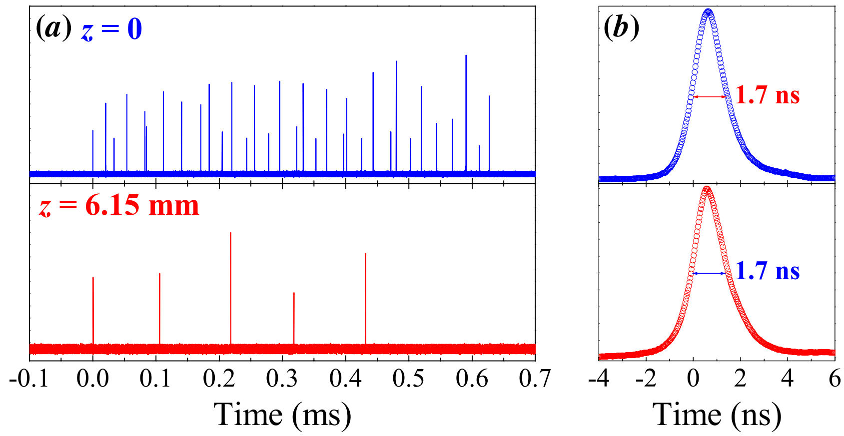

Figure 4. (*a*) Typical laser pulse trains of Nd:YAG/Cr^{4+}:YAG composite crystal passively Q-switched microchip laser at $z = 0$ and $z = 6.15$ mm. (*b*) The corresponding pulse profiles at $z = 0$ and $z = 6.15$ mm. (The colour version of this figure is included in the online version of the journal.)

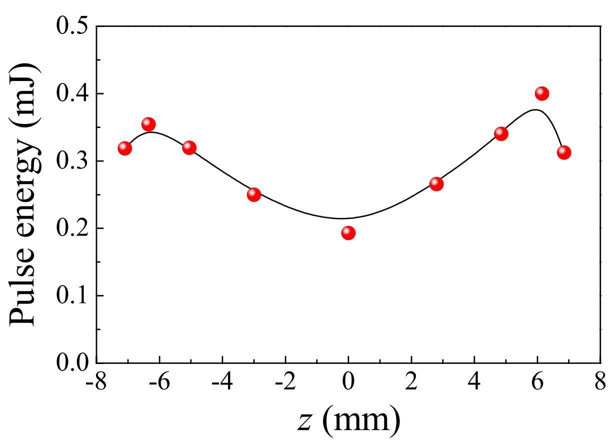

Figure 5. Q-switched pulse energy as a function of z (the position of the Nd:YAG/Cr^{4+}:YAG composite crystal along the pump beam direction). (The colour version of this figure is included in the online version of the journal.)

pump beam waist has a great effect on the number of laser pulses generated in Nd:YAG/Cr^{4+}:YAG composite crystal passively Q-switched microchip laser. The larger pump beam diameter causes low pump power intensity when the incident pump power level is set to constant; the population lifted to the upper laser state is decreased. Therefore, the time for accumulating sufficient inversion population for laser pulse oscillation is extended; the laser pulse number decreases within the same pump pulse duration.

Because the high pump peak power of QCW laser diode was applied in Nd:YAG/Cr^{4+}:YAG composite crystal passively Q-switched microchip laser, the pump power intensity was high enough to fulfill the intracavity photons to oscillate; therefore, the pulse width was kept nearly constant at different pump beam diameters. Figure 4 shows the laser pulse trains at $z = 0$ and $z = 6.15$ mm in the QCW laser diode-pumped Nd:YAG/Cr^{4+}:YAG composite crystal passively Q-switched microchip laser, together with the typical oscilloscope pulse profiles when the Nd:YAG/Cr^{4+}:YAG composite crystal is positioned at $z = 0$ and $z = 6.15$ mm. Within 0.7 ms pump pulse duration, 33 pulses were generated at $z = 0$, while 5 laser pulses were generated at $z = 6.15$ mm. Severe peak power fluctuation and time jitter between laser pulses were found at $z = 0$, while the fluctuation of the peak power and the time jitter between five laser pulses were dramatically alleviated when the Nd:YAG/Cr^{4+}:YAG composite crystal was moved to $z = 6.15$ mm. The repetition rates of laser pulses were determined to be 51 kHz at $z = 0$ and 9.3 kHz at $z = 6.15$ mm from Figure 4(*a*). The typical laser pulse generated at $z = 0$ and $z = 6.15$ mm in the Nd:YAG/Cr^{4+}:YAG composite crystal passively Q-switched laser is shown in Figure 4(*b*). The pulse profile at $z = 0$ is similar to that at $z = 6.15$ mm. And the pulse width is kept the same at both $z = 0$ and $z = 6.15$ mm. The laser pulse with pulse energy of 0.4 mJ and pulse width (FWHM) of 1.7 ns was obtained at $z = 6.15$ mm. Therefore, the peak power of Nd:YAG/Cr^{4+}:YAG composite crystal passively Q-switched laser is estimated to be over 235.3 kW.

The pulse energy of QCW laser diode-pumped Nd:YAG/Cr^{4+}:YAG composite crystal passively Q-switched laser as a function of z is shown in Figure 5. The Q-switched single pulse energy of 0.193 mJ was obtained at $z = 0$. The single pulse energy increases with $|z|$ when the Nd:YAG/Cr^{4+}:YAG composite crystal was moved away from $z = 0$. There are two optimal positions at $z = -6.35$ mm and $z = 6.15$ mm for achieving high pulse energy. However, highest pulse energy of 0.4 mJ was achieved at $z = 6.15$ mm, which was higher than 0.354 mJ obtained at $z = -6.35$ mm. The pulse energy at $z = 6.15$ mm is two times of that obtained at $z = 0$. Further moving Nd:YAG away from these two positions to increase the pump beam waist, the single pulse energy decreased.

The results shows that high pulse energy generation in the Nd:YAG/Cr^{4+}:YAG composite crystal passively Q-switched laser strongly depends on the position of Nd:YAG/Cr^{4+}:YAG composite crystal along the pump beam direction. High pulse energy can be generated by choosing a suitable position of the Nd:YAG/Cr^{4+}:YAG composite crystal along the pump beam direction, which opens a new window for designing high peak power passively Q-switched microchip lasers.

4. Theoretical model

The variation of the pulse energy with the position of Nd:YAG/Cr^{4+}:YAG composite crystal along the pump beam direction is attributed to the variation of the inversion population distribution inside Nd:YAG crystal, which strongly depends on the incident pump beam waist and the propagation of pump beam inside the Nd:YAG crystal. The output pulse energy of passively Q-switched laser is proportional to the effective laser beam area and can be expressed as follows [18–20],

$$E = \frac{h\nu A_{eff}}{2\sigma\gamma} \ln\left(\frac{N_i}{N_f}\right) \ln\left(\frac{1}{R_{OC}}\right) \quad (1)$$

where $h\nu$ is the laser photon energy, A_{eff} is the effective laser beam area, σ is the emission cross section of gain medium, γ is the inversion reduction factor of laser medium, and R_{OC} is the reflectivity of the output coupler. The initial inversion population, N_i, the threshold inversion population, N_{th}, and the final inversion population after pulse output, N_f, of Cr^{4+}:YAG passively Q-switched Nd:YAG microchip laser can be expressed as [21],

$$N_i = \left[2 \cdot \sigma_{gs} \cdot N_{s0} \cdot l_s + \ln\left(1/R_{OC}\right) + \delta_{Loss}\right] / (2 \cdot \sigma \cdot l) \quad (2)$$

$$N_{th} = \left[2 \cdot \sigma_{es} \cdot N_{s0} \cdot l_s + \ln\left(1/R_{OC}\right) + \delta_{Loss}\right] / (2 \cdot \sigma \cdot l) \quad (3)$$

$$N_i - N_f - N_{th} \cdot \ln\left(N_i / N_f\right) = 0 \quad (4)$$

where σ_{gs} and σ_{es} are the ground-state absorption cross section and excited-state absorption cross section of Cr^{4+}:YAG saturable absorber, N_{s0} is the total concentration of Cr^{4+} in Cr^{4+}:YAG crystal, l_s is the length of the Cr^{4+}:YAG crystal, l is the length of the Nd:YAG crystal, and δ_{Loss} is the total intracavity loss.

When the cavity parameters are set for Nd:YAG/Cr^{4+}:YAG composite crystal passively Q-switched microchip laser, the output energy mainly depends on the effective laser beam area, A_{eff}. The effective laser beam area, A_{eff}, is relative to the pump beam waist, pump power applied on the gain medium, and the initial inversion population needed for laser oscillation. When a focused pump beam from a laser diode is incident on Nd:YAG/Cr^{4+}:YAG composite crystal, the variation of pump beam waist with z along the pump beam propagation direction can be expressed as,

$$w_p(z) = w_0 \cdot \sqrt{1 + \frac{\left(M^2\right)^2 \cdot \lambda_p^2 \cdot \left(z - z_0\right)^2}{\pi^2 \cdot w_0^4 \cdot n^2}} \quad (5)$$

where w_0 is the focused pump beam waist at z_0, z_0 is the position of the focused pump beam waist, M^2 is the beam quality factor, n is the refractive index of gain medium, and λ_p is the pump wavelength. The incident pump beam waist (w_p) on the Nd:YAG/Cr^{4+}:YAG composite crystal can be varied by moving Nd:YAG/Cr^{4+}:YAG composite crystal along the pump beam direction, as shown in Figure 1. The spatial distribution of the population inversion, $\Delta N(r, z)$, along the thickness and radial direction inside the Nd:YAG crystal provided by the pump power can be expressed as,

$$\Delta N(r, z) = \frac{2P_{in}\alpha f_a \tau}{h\nu_p \pi w_p^2(z)} \exp\left(\frac{-2r^2}{w_p^2(z)}\right) \exp(-\alpha z) \quad (6)$$

where P_{in} is the incident pump power, r is the radial direction in the plane transverse to the laser propagation direction, z is the pump beam position incident on the Nd:YAG crystal along the laser propagation direction, h is the Planck constant, ν_p is the frequency of the pump power, τ is the fluorescence lifetime of gain medium, α is the absorption coefficient of gain medium at pump wavelength λ_p, f_a is the fractional equilibrium Boltzmann population of the upper laser level in the crystal field component, and $w_p(z)$ is the pump beam waist at position z.

The effective laser beam area is determined by the inversion population provided by the pump beam and the initial inversion population needed for oscillation of the Nd:YAG/Cr^{4+}:YAG composite crystal passively Q-switched microchip laser. It is reasonable to assume that the initial inversion population is constant when the intracavity laser intensity is high enough to bleach the Cr^{4+}:YAG saturable absorber. The inversion population distribution inside the Nd:YAG crystal strongly depends on the incident pump beam waist and incident pump power. Owing to the exponential decay of the pump power along the thickness of Nd:YAG crystal, the absorbed pump power decreases along the thickness of the Nd:YAG crystal. The pump power intensity along the thickness of Nd:YAG crystal depends on the incident pump beam waist applied. The inversion population distribution varies with the position

Table 1. The parameters of Nd:YAG/Cr^{4+}:YAG composite crystal passively Q-switched microchip laser used for theoretical calculation.

Parameter (unit)	Value	Reference
σ (cm^2)	2.3×10^{-19}	[22]
σ_{gs} (cm^2)	4.6×10^{-18}	[23–25]
σ_{es} (cm^2)	8.2×10^{-19}	[23]
τ (μs)	230	[22]
τ_s (μs)	3.4	[23]
γ	1	
$h\nu_p$ (J)	2.46×10^{-19}	
$h\nu$ (J)	1.87×10^{-19}	
l (mm)	3	
l_s (mm)	0.5	
R_{OC} (%)	60	
δ_{Loss}	0.1	
N_{s0} (cm^{-3})	9.66×10^{17}	
α (cm^{-1})	7	
P_{in} (W)	81	

inside Nd:YAG crystal. Therefore, in order to accurately evaluate the effective laser beam area, the Nd:YAG crystal is treated as many pieces of Nd:YAG crystal stacking together. For each piece of Nd:YAG crystal, it is reasonable to assume that the laser beam waist at the entrance surface is equal to that at the exit surface. The incident pump beam power and beam waist for each piece Nd:YAG crystal are estimated by applying the exponential decay law and the variation of the pump beam along the propagation direction of pump beam. Eventually, the effective laser beam area is obtained by averaging the laser beam area of different pieces of Nd:YAG crystal over the thickness of Nd:YAG crystal. When the Nd:YAG/Cr^{4+}:YAG composite crystal is set at position z along the pump beam direction, the effective laser beam area can be expressed as:

$$A_{eff} = \frac{1}{N}\sum_{i=1}^{N} \frac{\pi w_p^2(z+t_i)}{2} \ln \frac{2\tau P_{in}\alpha \exp(-\alpha t_i)}{N_i h\nu_p \pi w_p^2(z+t_i)} \quad (7)$$

where N is the number of Nd:YAG crystal slices and t_i is the position of i_{th} slice in Nd:YAG crystal ($t_i \in [0, l]$).

5. Discussion

The effective laser beam area, A_{eff}, is calculated according to Equation (7) with properly choosing the parameters of Nd:YAG, Cr^{4+}:YAG crystal, pump beam, and laser cavity based on the laser experiments. The parameters used for calculation of the effective beam area are listed in Table 1. Figure 6 shows the calculated effective laser beam area in QCW laser diode-pumped Nd:YAG/Cr^{4+}:YAG composite crystal passively Q-switched microchip laser versus the position of Nd:YAG/Cr^{4+}:YAG composite crystal along the pump beam direction for different focused pump beam waists. When the Nd:YAG/Cr^{4+}:YAG composite crystal is moved away from $z = 0$, the calculated effective laser beam area increases with the absolute value of z. There are two positions for achieving large effective laser beam area. The effective laser beam area decreases with further increase in the absolute values of z; this is caused by the decrease in the incident pump power intensity with further increase in the pump beam diameter applied on the Nd:YAG/Cr^{4+}:YAG composite crystal. For the focused pump beam waist of 0.3 mm used in the experiment, two positions of the Nd:YAG/Cr^{4+}:YAG composite crystal for achieving large effective laser beam area locate at $z = -9.5$ and 10.5 mm, respectively. When the Nd:YAG/Cr^{4+}:YAG composite crystal is located at $z = 0$, the effective laser beam area is only half of those at $z = -9.5$ and 10.5 mm. The pump beam focused waist has an effect on the effective laser beam area. The effective laser beam area at $z = 0$ increases with the focused pump beam waist. The peak effective laser beam area at $z < 0$ decreases with the focused pump beam waist, while the peak effective laser beam area at $z > 0$ increases a little with the focused pump beam waist. The position of the peak effective laser beam area expands with the focused pump beam waist.

Two peaks of the calculated effective laser beam area locating away from $z = 0$ are in good agreement with the pulse energy variation with the position of the Nd:YAG/Cr^{4+}:YAG composite crystal along the pump beam direction (as shown in Figure 5). However, there are some discrepancies between the variation of the calculated effective laser beam area and the pulse energy with the position of the Nd:YAG/Cr^{4+}:YAG composite crystal along the pump beam direction. The optimal position of the Nd:YAG/Cr^{4+}:YAG composite crystal along the pump beam direction to obtain highest pulse energy locates at $z = 6.15$ mm, while the largest effective laser beam area locates at $z = -9.5$ mm and the second largest effective laser beam area locates at $z = 10.5$ mm. The causes of the discrepancies between the experimental data and the calculated results are thermal effect and mode matching between pump beam and laser beam. The thermal effect was ignored in the simulation of the effective laser beam area. The thermal effect in the Nd:YAG/Cr^{4+}:YAG

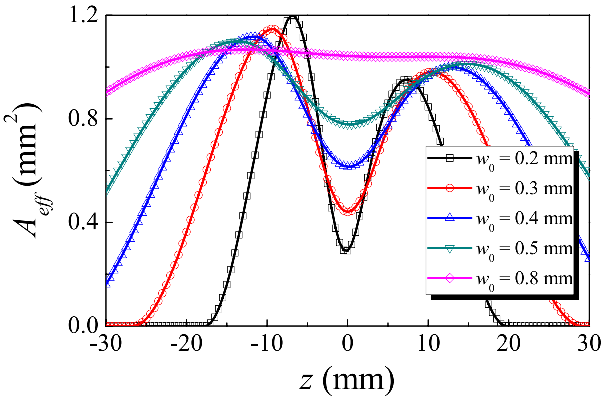

Figure 6. Theoretically calculated effective laser beam area as a function of z (the position of the Nd:YAG/Cr^{4+}:YAG composite crystal along the pump beam direction) for different focused pump beam waists. (The colour version of this figure is included in the online version of the journal.)

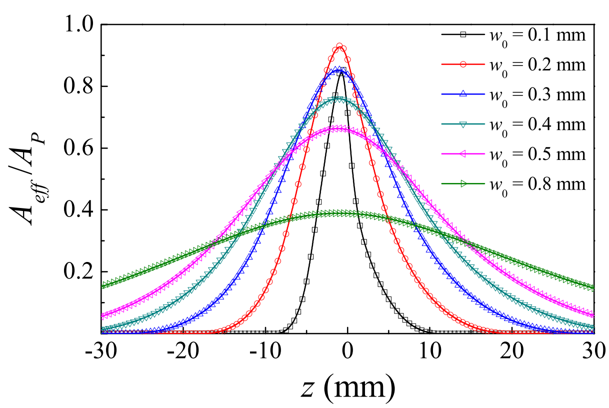

Figure 7. Mode matching between laser beam and pump beam of Nd:YAG/Cr^{4+}:YAG composite crystal passively Q-switched microchip laser as a function of z for different focused pump beam waists. (The colour version of this figure is included in the online version of the journal.)

composite crystal passively Q-switched laser is a main factor to limit the laser performance. The thermal effect degrades the emission cross section of Nd:YAG crystal and also increases the initial transmission of Cr^{4+}:YAG crystal, which limits the output energy from passively Q-switched lasers. The loss of the cavity was assumed to be a constant in the theoretical calculation; however, the pump beam area and laser beam area have great effects on the loss in practice. The variation of the cavity loss with pump beam area affects the accurate calculation of the N_i, N_{th}, and N_f. All of these factors have some influence on the accurate estimation of the effective laser beam area.

The mode matching between the laser beam and pump beam in the Nd:YAG/Cr^{4+}:YAG composite crystal passively Q-switched microchip laser was estimated by calculating the ratio of the laser beam area to the pump beam area. The ratio of the laser beam area to the pump beam area as a function of z for different focused pump beam waists is shown in Figure 7. The good mode matching is achieved around $z = -1$ mm for different focused pumped beam waists. The best mode matching is achieved at $z = -1$ mm for the focused pump beam waist of 0.2 mm, and the mode matching becomes worse with further increase in focused pump beam waist. The pump power intensity decreases with large pump beam waist. Only the pump beam area with the inversion population higher than the initial inversion population could support the laser oscillation. This means the optical efficiency is degraded with the pump beam waist. When the focused pump beam waist is smaller than 0.2 mm, the Rayleigh length of the focused pump beam is shortened and the effective laser beam area is decreased; therefore, the mode matching between laser beam and pump beam is also getting worse. The mode matching between laser beam and pump beam gets worse when the Nd:YAG crystal is moved away from $z = -1$ mm. The mode matching is getting worse dramatically with z away from $z = -1$ mm when the small pump beam waist is applied.

Based on the experimental results of the variation of the pulse energy with z and the calculated effective laser beam area with z, an optimal position of the Nd:YAG/Cr^{4+}:YAG composite crystal along the pump beam direction can be obtained for generating high pulse energy. There are two positions to achieve highest effective laser beam area for different focused pump beam waists, as shown in Figure 6. The focused pump beam waist affects the effective laser beam area. The smaller the focused pump beam waist used, the more obvious influence of z on the effective laser beam area, A_{eff}. For the cases of w_0 = 0.3 mm and w_0 = 0.8 mm, the variation of the effective laser beam area, A_{eff}, with z is significantly different. The variation of the A_{eff} with the absolute value of z tends to be stable in a large range for w_0 = 0.8 mm; the difference between the peaks and valley tends to be negligible. Namely, the optimal position of Nd:YAG/Cr^{4+}:YAG composite crystal for achieving high pulse energy is flexible. However, the optical efficiency degrades because the pump beam waist is too large to support large laser beam area and the mode matching becomes worse. Only when a fraction of the pump beam area can be excited for laser oscillation, the mode matching is worsened. For the small focused pump beam waist such as w_0 = 0.3 mm, the highest laser beam area can be obtained by adjusting the position of the Nd:YAG/Cr^{4+}:YAG composite crystal along the pump beam direction, as shown in Figure 6. Besides the larger effective laser beam area, the high pump power intensity and good mode matching between laser beam and pump beam can be maintained even moving Nd:YAG/Cr^{4+}:YAG composite crystal away from $z = 0$; therefore, high pulse energy and the high optical efficiency could be achieved.

This is important for designing highly efficient, high peak power passively Q-switched solid-state lasers by applying suitable pump beam parameters.

6. Conclusions

The effects of the incident pump beam waist on the pulse energy generation in the Nd:YAG/Cr^{4+}:YAG composite crystal passively Q-switched microchip laser have been investigated experimentally and theoretically. The highest pulse energy is obtained by optimizing the position of the Nd:YAG/Cr^{4+}:YAG composite crystal along the pump beam direction. Two optimal positions with suitable incident pump beam waist incident on the Nd:YAG/Cr^{4+}:YAG composite crystal give largest effective laser beam area for high pulse energy generation in passively Q-switched microchip lasers. The variation of the effective laser beam area with the position of the Nd:YAG/Cr^{4+}:YAG composite crystal is in good agreement with the experimentally obtained incident pump beam waist-dependent pulse energy. Laser pulses with pulse energy of 0.4 mJ, pulse width of 1.7 ns, and peak power of 235.3 kW have been obtained by setting Nd:YAG/Cr^{4+}:YAG composite crystal at z = 6.15 mm along the pump beam direction. The experimental results and theoretical simulation of position-dependent high pulse energy generation in Nd:YAG/Cr^{4+}:YAG composite crystal passively Q-switched microchip laser provide a new method for designing end-pumped passively Q-switched solid-state lasers for high peak power generation without sacrificing the optical efficiency.

Acknowledgements

This work was supported by the National Natural Science Foundation of China under [grant number 61275143] and [grant number 61475130]; the Program for New Century Excellent Talents in University under [grant number NCET-09-0669].

Disclosure statement

No potential conflict of interest was reported by the authors.

References

[1] Zayhowski, J.J. *Laser Focus World*. **1999**, *35*, 129–136.
[2] Kofler, H.; Tauer, J.; Tartar, G.; Iskra, K.; Klausner, J.; Herdin, G.; Wintner, E. *Laser Phys. Lett.* **2007**, *4*, 322–327.
[3] Tsunekane, M.; Inohara, T.; Ando, A.; Kido, N.; Kanehara, K.; Taira, T. *IEEE J. Quantum Electron.* **2010**, *46*, 277–284.
[4] Kalisky, Y.; Kravchik, L.; Kokta, M.R. *Opt. Mater.* **2004**, *24*, 607–614.
[5] Pavel, N.; Tsunekane, M.; Taira, T. *Opt. Express*. **2011**, *19*, 9378–9384.
[6] Salamu, G.; Ionescu, A.; Brandus, C.A.; Sandu, O.; Pavel, N.; Dascalu, T. *Laser Phys.* **2012**, *22*, 68–73.
[7] Sakai, H.; Kan, H.; Taira, T. *Opt. Express*. **2008**, *16*, 19891–19899.
[8] Sandu, O.; Salamu, G.; Pavel, N.; Dascalu, T.; Chuchumishev, D.; Gaydardzhiev, A.; Buchvarov, I. *Quantum Electron.* **2012**, *42*, 211–215.
[9] Wang, H.X.; Yang, X.Q.; Zhao, S.; Zhang, B.T.; Huang, H.T.; Yang, J.F.; Xu, J.L.; He, J.L. *Laser Phys.* **2009**, *19*, 1824–1827.
[10] Dong, J.; Ueda, K.; Shirakawa, A.; Yagi, H.; Yanagitani, T.; Kaminskii, A.A. *Opt. Express*. **2007**, *15*, 14516–14523.
[11] Dong, J.; Ren, Y.Y.; Cheng, H.H. *Laser Phys.* **2014**, *24*, 055801.
[12] Degnan, J.J. *IEEE J. Quantum Electron.* **1989**, *25*, 214–220.
[13] Lin, Z.; Gao, C.; Gao, M.; Zhang, Y.; Weber, H. *Appl. Phys. B*. **2009**, *94*, 81–84.
[14] Liu, X.; Klinkhammer, S.; Wang, Z.; Wienhold, T.; Vannahme, C.; Jakobs, P.-J.; Bacher, A.; Muslija, A.; Mappes, T.; Lemmer, U. *Opt. Express*. **2013**, *21*, 27697–27706.
[15] Hwong, S.L.; Tsai, W.L.; Lim, T.S.; Chern, J.L. *Jap. J. Appl. Phys.* **1999**, *38*, L1330–L1332.
[16] Kim, H.S.; Yang, J.M.; Lim, C. *J. Korean Phys. Soc.* **2009**, *55*, 1425–1429.
[17] Helmfrid, S.; Andou, T.; Nakatsuka, S.; Tatsuno, K. *Opt. Rev.* **1995**, *2*, 199–203.
[18] Dong, J.; Lu, J.R.; Ueda, K. *J. Opt. Soc. Am. B* **2004**, *21*, 2130–2136.
[19] Zhang, X.Y.; Zhao, S.Z.; Wang, Q.P.; Zhang, Q.D.; Sun, L.K.; Zhang, S.J. *IEEE J. Quantum Electron.* **1997**, *33*, 2286–2294.
[20] Degnan, J.J. *IEEE J. Quantum Electron.* **1995**, *31*, 1890–1901.
[21] Dong, J. *Opt. Commun.* **2003**, *226*, 337–344.
[22] Dong, J.; Rapaport, A.; Bass, M.; Szipocs, F.; Ueda, K. *Phys. Status Sol. A*. **2005**, *202*, 2565–2573.
[23] Burshtein, Z.; Blau, P.; Kalisky, Y.; Shimony, Y.; Kokta, M.R. *IEEE J. Quantum Electron.* **1998**, *34*, 292–299.
[24] Xiao, G.; Lim, J.H.; Yang, S.; Stryland, E.V.; Bass, M.; Weichman, L. *IEEE J. Quantum Electron.* **1999**, *35*, 1086–1091.
[25] Lipavsky, B.; Kalisky, Y.; Burshtein, Z.; Shimony, Y.; Rotman, S. *Opt. Mater.* **1999**, *13*, 117–127.